

Surface Texturing of TiO₂ Film by Mist Deposition of TiO₂ Nanoparticles

Gang Qin^{1,2}, Akira Watanabe^{1,*}

(Received 22 April 2013; accepted 13 June 2013; published online 30 June 2013)

Abstract: Unique and various microstructures of titanium oxide (TiO₂) film including macroporous structure, chromatic veins and rings, have been easily fabricated by mist deposition method on silicon substrate with mild preparation conditions. Rutile phase TiO₂ nanoparticles were directly used as starting material to prepare film and led to a simple preparation process. It was found that several different microstructures existed in the sample and changed with the varied positions from the center to the edge of the film when the concentration of the TiO₂ suspension is 0.06 mol/l, the deposition time is 30 min, the flow rate is 1 l/min and the temperature is 150°C. The surface texturing shows apparent distinction as the concentration of the TiO₂ suspension decreased to 0.03 mol/l and 0.01 mol/l.

Keywords: Mist deposition; TiO₂ film; TiO₂ nanoparticle; Surface texturing; Microstructure

Citation: Gang Qin and Akira Watanabe, "Surface Texturing of TiO₂ Film by Mist Deposition of TiO₂ Nanoparticles", *Nano-Micro Lett.* 5(2), 129-134 (2013). <http://dx.doi.org/10.5101/nml.v5i2.p129-134>

Introduction

There has been great interest in titanium oxide (TiO₂) film due to its chemical stability, high transparency in the visible region, photocatalytic activity and great mechanical durability. The main applications of TiO₂ films are in solar cells [1], gas sensors [2], optical coatings [3], photo-catalytic systems [4], and other devices. For many applications, porous TiO₂ films have attracted considerable attention because of large surface areas [5], highly ordered porous structures [6], and well-defined pore sizes and porosity [7]. There are various preparation methods of porous TiO₂ films such as sol-gel method [8], templating assembly method [9], reverse micelle [10], spray-pyrolysis method [11], aerosol deposition [12] and cathodic electrodeposition [13].

Different from these manufacture techniques, mist deposition has outstanding potential for the development of film with some advantages such as easy and atmospheric operation, simple structure, cheapness etc [14]. A film can be efficiently obtained with rapid depo-

sition rate on large area, even rough and diverse substrate such as polymer, silicon, glass and metal. Because of its ability of being used under low temperature, mist deposition method has more practical value to prepare TiO₂ film whose crystal form depends on the temperature in a great extent. Up to now, there is no literature report about the preparation of porous TiO₂ film by mist deposition method. For an efficient light trapping in the thin-film solar cell, the textured back reflector which will scatter the light backward resulting in an increase in light path in the absorber layer is verified to be an effective technique to enhance photoelectric conversion efficiency. Such TiO₂ film can be applied as a textured reflector due to the rough surface and the high reflective index of TiO₂. In this paper, we report the novel technique to prepare TiO₂ films with unique surface textures possessing not only porous structure but also ring and chromatic veins by mist deposition method using nanoparticles as starting material at a low temperature. The influence of the concentration of TiO₂ nanoparticles suspension on thickness and mor-

¹Institute of Multidisciplinary Research for Advanced Materials, Tohoku University, Sendai 980-8577, Japan

²School of Materials Science and Engineering, Henan Polytechnic University, Jiaozuo 454001, China

*Corresponding author. E-mail: watanabe@tagen.tohoku.ac.jp

phology of film was investigated. In comparison with the uniform TiO₂ porous films obtained by other methods, the randomly textured TiO₂ film prepared by mist deposition is more suitable for our research purpose because its roughness is high and the angular dependence of reflectance is low on random surface and more incident light can be scattered in the solar cell if such kind of textured TiO₂ film used as back reflector.

Experimental

The mist deposition process was performed in a self-designed apparatus shown in Fig. 1. The deposition apparatus mainly consists of an atomizing system, a tube, and a heater chamber. For deposition of films, TiO₂ nanoparticles suspension (TK-535, 23.6 wt% TiO₂ unit, rutile crystal form, Tayca Corp., contains 0.7 wt% HNO₃ as the stabilizer) was diluted by water to a certain concentration as the precursor. After the chamber and substrate were heated to 150°C, the mist of TiO₂ nanoparticles suspension was atomized by ultrasonic power of transducer (frequency: 2.5 MHz) equipped at the bottom of the solution container, transported into the chamber by N₂ carrier gas through a tube of 60°C, and then the mist filled in the chamber and deposited on the substrate. When the frequency of the ultrasonic transducer is 2.5 MHz, the diameter of mist droplet is about 3 μm [15]. A p-type (100) silicon substrate and a glass substrate were used in our experiment, and before being used the silicon one was irradiated by deep UV (Photo surface processor, PL16-110, Sen Light Corp.) for 20 min to introduce hydroxyl group on their surface in order to increase the hydrophilicity and to improve the binding force of substrate/TiO₂ nanoparticles. The flow rate was controlled by a glass flowmeter. The mist flow was introduced to a cone-shape nozzle through an epoxy tube, both of which have the inner diameter of 4.2 mm. Then mist deposition was carried out from the cone-shape nozzle to a substrate, and the distance between them is 29.5 mm. All the procedures were carried out under 1 atm of pressure.

In contrast, a flat TiO₂ film was prepared by spin

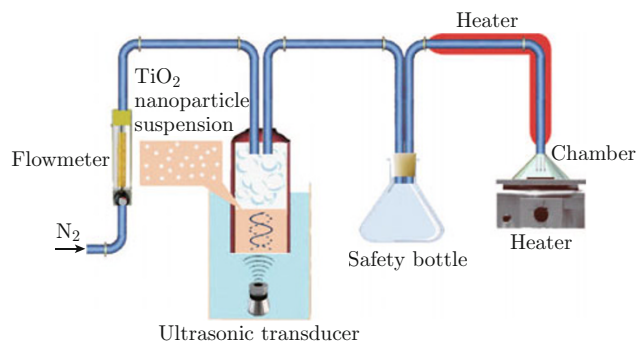


Fig. 1 Reactor illustration for mist deposition method.

coating method on the glass substrate. The TK-535 TiO₂ nanoparticles suspension was diluted by water to 10 wt%. Spin coating was carried out using a spin coater (MS-A100, Mikasa Co., Ltd) with a rate of 2000 rpm for 30s at RT in air.

The surface morphology and thickness of the film were investigated using a violet laser scanning microscope (VK 9700, Keyence Corp.) and a scanning electron microscope (XL30, Philips Electronic N.V.), and the structure of TiO₂ nanoparticles were detected by micro-Raman spectroscopy.

Results and discussion

The characteristic of the TiO₂ film was investigated by micro-Raman spectroscopy with the measurement area indicated by Fig. 3(b) as the typical case, and no difference in the micro-Raman spectra was observed with the measurement area changing. Figure 2 is the Raman shifts exhibiting dominant peaks at 140.2, 246.1, 449.5, and 615.7 cm⁻¹ which can be assigned as the Raman active modes of rutile crystal phase: *B*_{1g}, multi-photon process, *E*_g, and *A*_{1g}, and the numbers and frequencies of the Raman bands coincide with previous studies [16]. The peak of 1060 cm⁻¹ is attributed to NO₃⁻ of the stabilizer HNO₃.

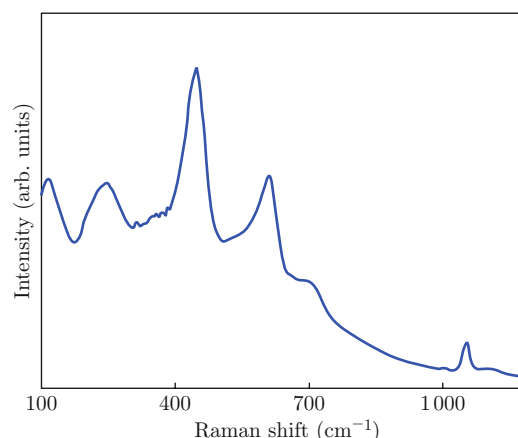


Fig. 2 Micro-Raman spectrum of TiO₂ nanoparticles.

A circular white film formed on the substrate when the concentration of suspension based on TiO₂ unit is 0.06 mol/l, the deposition time is 30 min and the flow rate is 1 l/min. The morphologies showed a remarkable dependence on the viewing areas of sample, in other words, the morphologies depend on the thickness of the film. The micrographs and 3D images of the TiO₂ film observed by laser scanning microscope at varied positions are shown in Fig. 3. In the center of sample (Fig. 3(a)), there is a thick, flat and white film with the thickness of about 11.4 μm and the root mean square roughness (*R*_q) of 0.21 μm. At the site of 843 μm from

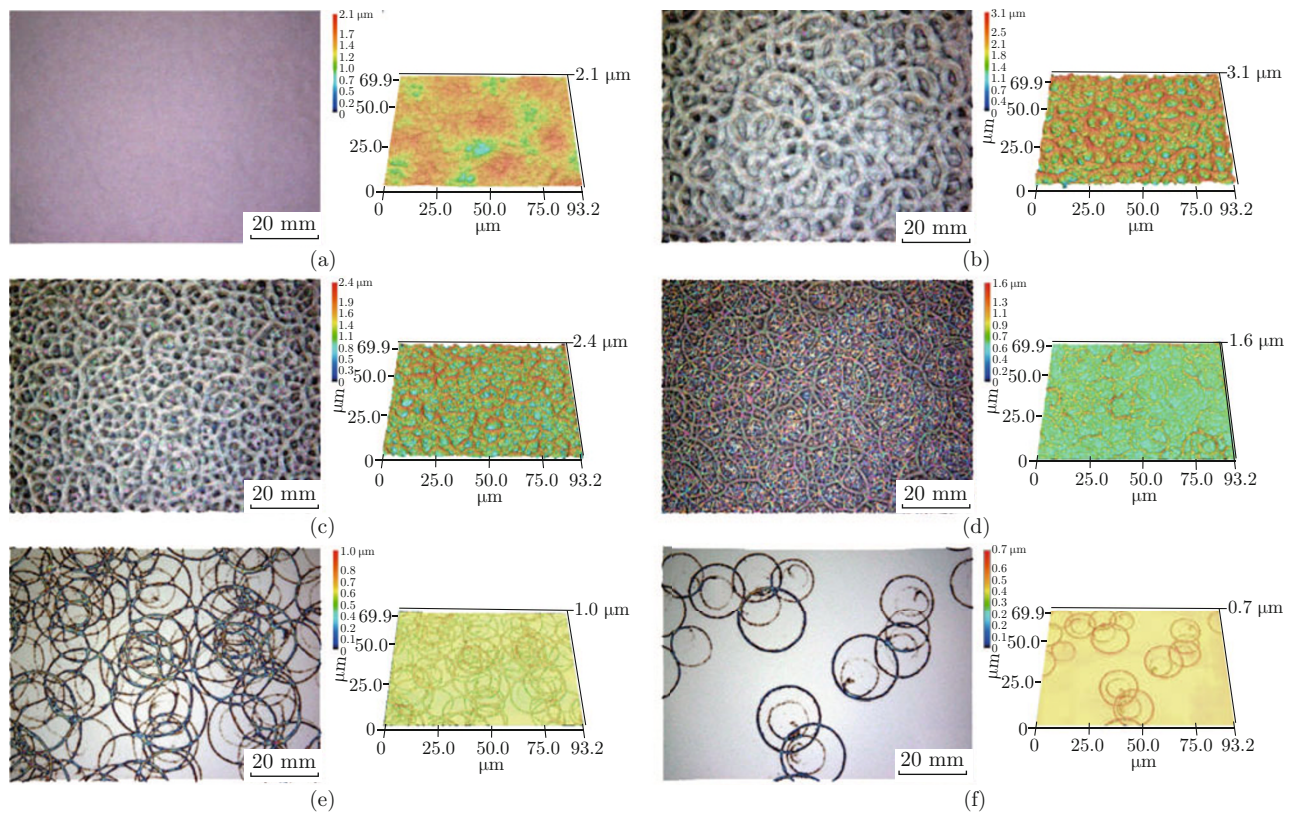


Fig. 3 Surfaces and 3D images obtained at different positions of the TiO_2 film prepared by mist deposition method.

the center (Fig. 3(b)), there are some pores and raised, crossed and white lines like veins on the film, where the depths of the pores are $1.22\sim 1.63\ \mu\text{m}$ and the diameters are estimated to be $2.38\sim 6.21\ \mu\text{m}$. The thickness of film is approximately $4.73\ \mu\text{m}$, the width of vein about $2.15\ \mu\text{m}$ and the R_q is $0.5\ \mu\text{m}$ which means that this film is rougher than other textured films previously reported [17]. A little farther away, about $1236\ \mu\text{m}$ from the center (Fig. 3(c)), the bottom of the pore becomes chromatic due to the interference phenomenon of light occurring when the bottom is enough thin. The depth and diameter of the pore are similar to image b, while the thickness of the film decreases to $1.34\ \mu\text{m}$, the vein width is approximately $1.89\ \mu\text{m}$, and the R_q is $0.39\ \mu\text{m}$. When the viewing area continues to move to the edge of the sample and is $1833\ \mu\text{m}$ from center, it can be observed that chromatic veins and bottom appeared (Fig. 3(d)). The thickness of the film is about $160\ \text{nm}$ and the bottom is approximately $67\ \text{nm}$. The lines of veins become thinner to $0.88\ \mu\text{m}$ and R_q is $0.14\ \mu\text{m}$. More close to the edge about $2937\ \mu\text{m}$ from center (Fig. 3(e)), there are many colorized rings with the thickness in $96\sim 138\ \text{nm}$ range and the diameter $17.01\sim 23.93\ \mu\text{m}$ on the substrate. On the edge of sample $3672\ \mu\text{m}$ off the center (Fig. 3(f)), only several separated rings can be observed, the thickness of which changes from $71\ \text{nm}$ to $136\ \text{nm}$ gradually, and the diameter is in the range of $14.35\sim 20.16\ \mu\text{m}$. Because the

diameter of the mist is about $3\ \mu\text{m}$ which is obviously smaller than that of the ring, the extension of it as a result of its flattening must be caused after the deposition on the substrate. TiO_2 nanoparticles were transferred to the edge of the flattening droplet from the drop point, and then the nanoparticles were fixed on the edge by the interaction with the substrate accompanying the evaporation of the water. The distribution of the ring size as shown in Fig. 3(f) is narrow due to the homogeneity of the mist size which depends on the frequency of a transducer. The overlapping of the ring structure of TiO_2 nanoparticles forms the porous structure as shown in Figs. 3(b), 3(c), and 3(d) with the film thickness increasing. Such roughness remarkably influenced the reflectance properties of the film. The angular dependence of the reflectance of the textured TiO_2 film on a glass substrate was compared with a TiO_2 nanoparticles film prepared by spin coating method. The decrease of the reflectance of the textured TiO_2 at $600\ \text{nm}$ was ca. 40% whereas that of a flat TiO_2 spin-coated film was 99.48% at 10° between the incident light and perpendicular of film surface. This result means that the textured TiO_2 film formed by mist deposition has the potential to be applied as a reflector.

The concentration of TiO_2 nanoparticles as the significant affecting factor on the morphology was investigated as shown in Fig. 4. When the concentration of suspension decreased, different surface texturing could

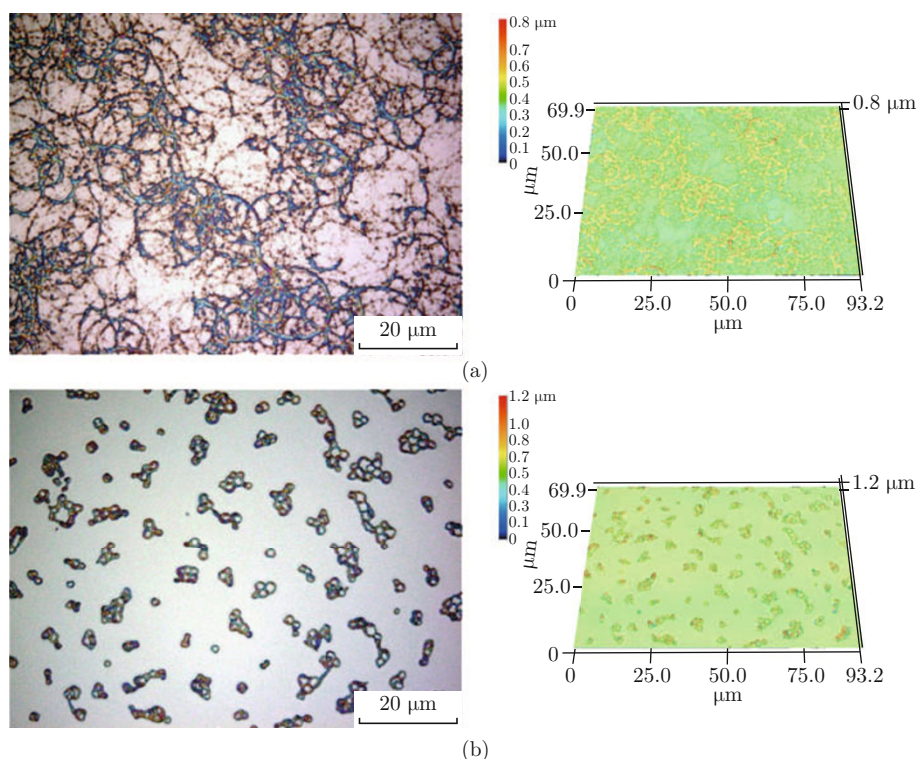


Fig. 4 Influences of the concentration of TiO_2 nanoparticles on the surface and 3D images of the film prepared by mist deposition method: (a) 0.03, (b) 0.01 mol/l.

be observed by laser scanning microscope. Figure 4(a) depicts the typical morphology of the sample gotten with the concentration of 0.03 mol/l. It can be seen that some disordered and discontinuous rings appeared and part of the ring is white but the other part is fuscous due to the difference of the thickness. The thickness of white part of the ring is in the range of 70~109 nm while fuscous part is approximately 33~42 nm, and the diameters is about 19.9~20.79 μm . When the concentration was further reduced to 0.01 mol/l, a structure of some connected small chromatic rings was observed as shown in Fig. 4(b), whose thickness is 105 nm, external diameter about 1.13~3.02 μm and width 504 nm. In the case of the droplet with a low concentration of TiO_2 nanoparticles, the aggregation of the nanoparticles does not occur remarkably on the edge of the flattening droplet, and then nanoparticles return the drop point with contraction of the flattening droplet. Two connected rings would be formed if a droplet deposited on the substrate adjoining another one previously formed. The morphology as shown in Fig. 4a presents an intermediate case, where there are aggregated and non-aggregated nanoparticles. The aggregated nanoparticles form a ring structure and the non-aggregated nanoparticles form a disordered structure inside the ring.

A close examination of the microstructure has been carried out by SEM. Figure 5(a) and 5(b) were taken from the same position as Fig. 3(b), indicating that

there are many blind-holes in the film like lotus seed pod structure. Figure 5(c) and 5(d) exhibit the images of separated ring shown in Fig. 3(f) and it can be observed that the nanoparticles are in short rod-like shape with length of approximately 80~90 nm and width of 25~35 nm. Judging from the SEM images, the shape and size are almost uniform and the nanoparticles are monodisperse particles. If Fig. 4(b) is enlarged by SEM, we can get the images like Fig. 5(e) and 5(f) in which some connected rings exist. Contrast to Fig. 5(c) and 5(d), this kind of ring is not regular and the diameter is smaller.

Conclusion

Using rutile phase TiO_2 nanoparticles as a starting material, we demonstrated the successful formation of porous TiO_2 films by the mist deposition method which is effective, inexpensive, easily-operated and practical at the temperature as low as 150°C and the pressure of 1 atm. Additional advantages of the mist deposition method using nanoparticles as starting material include the controllability of the microstructure and the surface texturing of film. Some unique and various microstructures of TiO_2 could be formed, such as macroporous structure, chromatic veins and rings. The significant varying surface morphology including irregular rings and small chromatic rings can be gotten as the concentration of TiO_2 nanoparticles suspension decreases.

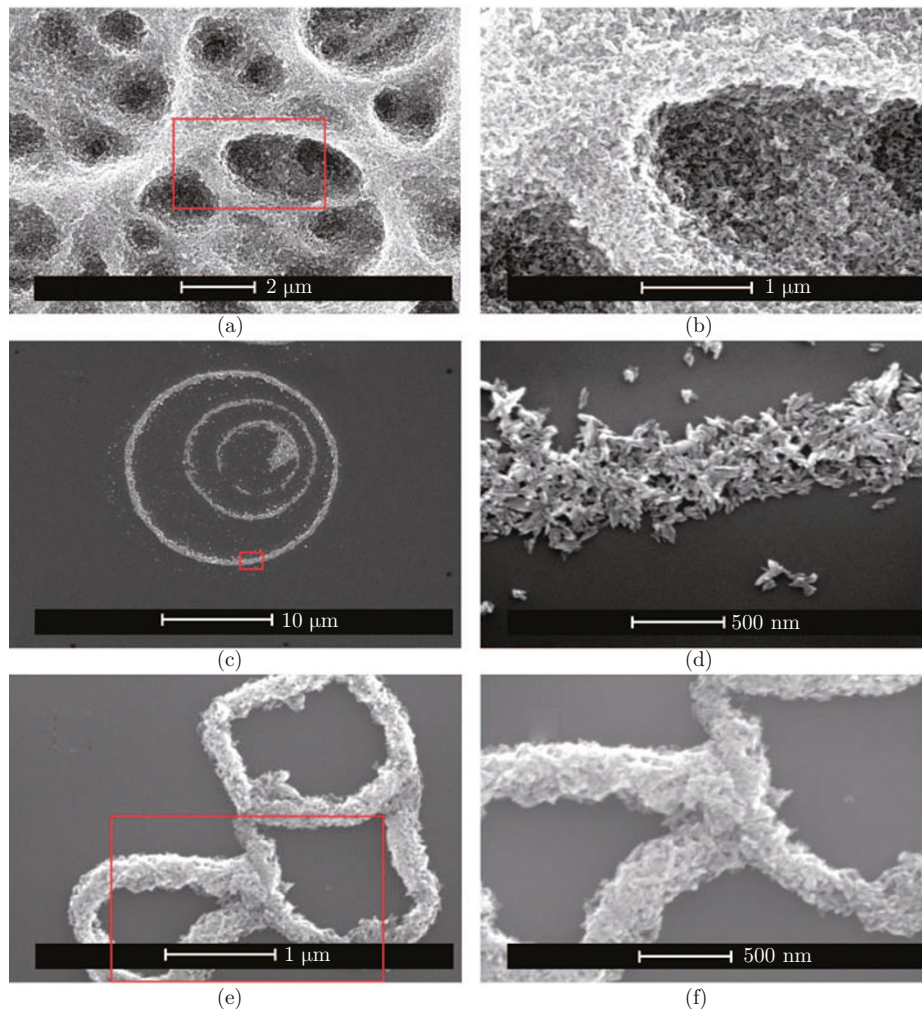


Fig. 5 SEM images of the surface textures of TiO₂ film prepared by mist deposition method.

Acknowledgments

This work was supported by a Grant-in-Aid for Scientific Research on Innovative Areas “New Polymeric Materials Based on Element-Blocks (No. 2401)” (24102004) of The Ministry of Education, Culture, Sports, Science, and Technology, Japan.

References

- [1] C. P. Kang, Z. X. Zhang, Y. Z. Zhang, Y. M. He, Xie and E. Q. Xie, “Enhanced efficiency in dye-sensitized solar cells using a TiO₂-based sandwiched film as photoanode”, *Micro Nano Lett.* 6(8), 579-581 (2011). <http://dx.doi.org/10.1049/nml.2011.0225>
- [2] M. A. Ponce, R. Parra, R. Savu, E. Joanni, P. R. Bueno, M. Cilense, J. A. Varela and M. S. Castro, “Impedance spectroscopy analysis of TiO₂ thin film gas sensors obtained from water-based anatase colloids”, *Sensor Actuat. B: Chem.* 139(2), 447-452 (2009). <http://dx.doi.org/10.1016/j.snb.2009.03.066>
- [3] W. X. Que, Z. Sun, Y. Zhou, Y. L. Lam, S. D. Cheng, Y. C. Chan and C. H. Kam, *Mater. Lett.* 42, 326 (2000). [http://dx.doi.org/10.1016/S0167-577X\(99\)00207-4](http://dx.doi.org/10.1016/S0167-577X(99)00207-4)
- [4] W. Y. Zhao, W. Y. Fu, H. B. Yang, C. J. Tian, M. H. Li, J. Ding, W. Zhang, X. M. Zhou, H. Zhao and Y. X. Li, “Synthesis and photocatalytic activity of Fe-doped TiO₂ supported on hollow glass microbeads”, *Nano-Micro Lett.* 3(1), 20-24 (2011). <http://dx.doi.org/10.3786/nml.v3i1.p20-24>
- [5] L. Wan, M. C. Long, D. Y. Zhou, L. Y. Zhang and W. M. Cai, “Preparation and characterization of free-standing hierarchical porous TiO₂ monolith modified with graphene oxide”, *Nano-Micro Lett.* 4(2), 90-97 (2012). <http://dx.doi.org/10.3786/nml.v4i2.p90-97>
- [6] H. Li, Y. Zhou, C. X. Lv and M. M. Dang, “Templated synthesis of ordered porous TiO₂ films and their application in dye-sensitized solar cell”, *Mater. Lett.* 65(12), 1808-1810 (2011). <http://dx.doi.org/10.1016/j.matlet.2011.03.044>
- [7] A. B. Dros, D. Grosso, C. Boissière, G. J. A. A. Soler-Illia, P. A. Albouy, H. Amenitsch and

- C. Sanchez, "Niobia-stabilised anatase TiO₂ highly porous mesostructured thin films", *Micropor. Mesopor. Mater.* 94(1-3), 208-213 (2006). <http://dx.doi.org/10.1016/j.micromeso.2006.03.034>
- [8] G. Q. Li, Z. G. Jin, X. X. Liu, T. Wang and Z. F. Liu, "Anatase TiO₂ porous thin films prepared by sol-gel method using CTAB surfactant", *J. Sol-Gel Sci. Techn.* 41(1), 49-55 (2007). <http://link.springer.com/article/10.1007/s10971-006-0122-9>
- [9] Z. Lan, J. H. Wu, J. M. Lin and M. L. Huang, "PF127 aided preparation of super-porous TiO₂ film used in highly efficient quasi-solid-state dye-sensitized solar cell", *J. Mater. Sci. Mater. Electron.* 21(10), 1000-1004 (2012). <http://dx.doi.org/10.1007/s10854-010-0083-1>
- [10] J. C. Yu, J. G. Yu and J. C. Zhao, "Enhanced photocatalytic activity of mesoporous and ordinary TiO₂ thin films by sulfuric acid treatment", *Appl. Catal. B: Environmental* 36(1), 31-43 (2002). [http://dx.doi.org/10.1016/S0926-3373\(01\)00277-6](http://dx.doi.org/10.1016/S0926-3373(01)00277-6)
- [11] O. Sugiyama, M. Okuya and S. Kaneko, "Photocatalytic ability of TiO₂ porous film prepared by modified spray pyrolysis deposition technique", *J. Ceram. Soc. Jpn.* 117, 203-207 (2009). <http://dx.doi.org/10.2109/jcersj2.117.203>
- [12] J. Ryu, B. D. Hahn, J. J. Choi, W. H. Yoon, B. K. Lee, J. H. Choi and D. S. Park, "Porous photocatalytic TiO₂ thin films by aerosol deposition", *J. Am. Ceram. Soc.* 93(1), 55-58 (2010). <http://dx.doi.org/10.1111/j.1551-2916.2009.03391.x>
- [13] S. Karuppuchamy, K. Nonomura, T. Yoshida, T. Sugiyama and H. Minoura, "Cathodic electrodeposition of oxide semiconductor thin films and their application to dye-sensitized solar cells", *Solid State Ionics* 151(1-4), 19-27 (2002). [http://dx.doi.org/10.1016/S0167-2738\(02\)00599-4](http://dx.doi.org/10.1016/S0167-2738(02)00599-4)
- [14] J. G. Lu, T. Kawaharamura, H. Nishinaka, Y. Kamada, T. Ohshima and S. Fujita, "ZnO-based thin films synthesized by atmospheric pressure mist chemical vapor deposition", *J. Cryst. Growth* 299(1), 1-10 (2007). <http://dx.doi.org/10.1016/j.jcrysgro.2006.10.251>
- [15] P. Singh, A. Kumar, Deepak and D. Kaur, "ZnO nanocrystalline powder synthesized by ultrasonic mist-chemical vapour deposition", *Opt. Mater.* 30(8), 1316-1322 (2008). <http://dx.doi.org/10.1016/j.optmat.2007.06.012>
- [16] A. Naumenko, I. Gnatiuk, N. Smirnova and A. Eremenko, "Characterization of sol-gel derived TiO₂/ZrO₂ films and powders by Raman spectroscopy", *Thin Solid Films*, 520(14), 4541-4546 (2005). <http://dx.doi.org/10.1016/j.tsf.2011.10.189>
- [17] W. Thongsuwan, T. Kumpika and P. Singjai, "Effect of high roughness on a long aging time of superhydrophilic TiO₂ nanoparticle thin films", *Curr. Appl. Phys.* 11(5), 1237-1242 (2011). <http://dx.doi.org/10.1016/j.cap.2011.03.002>